International Journal of Pharmaceutics 397 (2010) 184–193

Contents lists available at ScienceDirect

International Journal of Pharmaceutics

journal homepage: www.elsevier.com/locate/ijpharm

Pharmaceutical Nanotechnology

Liposomes loaded with histone deacetylase inhibitors for breast cancer therapy

Giorgia Urbinati[a,b], Véronique Marsaud[a,c], Vincent Plassat[a,c], Elias Fattal[a,b,c], Sylviane Lesieur[a,c], Jack-Michel Renoir[a,c,*]

[a] Centre National de la Recherche Scientifique, UMR 8612, Faculté de Pharmacie, 5 rue J.B. Clément, Châtenay-Malabry, F-92296, France
[b] Paris-SudUniversity, Orsay, F-91405, France
[c] IFR 141, Châtenay-Malabry, F-92296, France

ARTICLE INFO

Article history:
Received 26 March 2010
Received in revised form 23 June 2010
Accepted 24 June 2010
Available online 23 July 2010

Keywords:
HDAC inhibitors
Stealth® liposomes
Breast cancer
Estrogen receptor

ABSTRACT

Histone deacetylase (HDAC) inhibitors (HDACi) of the class I trichostatin A (TSA), CG1521 (CG), and PXD101 (PXD) were incorporated at a high rate (~1 mM) in liposomes made of egg phosphatidylcholine/cholesterol/distearoylphosphoethanolamine-polyethylenglycol$_{2000}$ (64:30:6). Physicochemical parameters (size, zeta potential, loading, stability, release kinetics) of these HDACi-loaded pegylated liposomes were optimized and their cytotoxicity (MTT test) was measured in MCF-7, T47-D, MDA-MB-231 and SkBr3 breast cancer cell lines. In MCF-7 cells, TSA and PXD were efficient inducers of proteasome-mediated estradiol receptor α degradation and they both affected estradiol-induced transcription (TSA > PXD) contrary to CG. Moreover, TSA most efficiently altered breast cancer cell viability as compared to the free drug, CG-liposomes being the weakest, while unloaded liposomes had nearly no cytotoxicity. Pegylated liposomes loaded with TSA or PXD remained stable in size, charge and biological activity for one month when stored at 4 °C. All HDACi-loaded liposomes released slowly the encapsulated drug *in vitro*, CG-loaded liposomes showed the slowest release kinetic. These formulations could improve the efficacy of HDACi not only in breast cancers but also in other solid tumors because most of these drugs are poor water soluble and unstable *in vivo*, and their administration remains a challenge.

1. Introduction

Acetylation and deacetylation of histones have important roles in the modulation of chromatin topology and in regulating transcription in many tumor cell types. Transcriptionally active chromatin is generally associated with hyperacetylated histones, while silenced chromatin, in its condensed state, is linked to hypoacetylated histones (Nightingale et al., 2006; Wade et al., 1997). Histone deacetylase inhibitors (HDACi[1]) are a new class of antitumor agents which induces histone hyperacetylation and inhibits the proliferation of tumor cells by inducing cell cycle arrest, differentiation and/or apoptosis (Grunstein, 1997; Marks et al., 2000). Moreover, non-histone proteins, such as transcription factors like nuclear steroid hormone receptors, particularly the estrogen receptor alpha (ERα) (Vigushin et al., 2001) and the tumor suppressor p53 (Roy et al., 2005) are also targets for acetylation with varying functional effects. Several laboratories have shown that in response to HDAC inhibition, certain genes such as the *CDKN1A* gene (Huang et al., 2000), which encodes the p21$^{WAF1/CIP1}$ cyclin dependent kinase inhibitor are activated but others such as the *CCDN1* gene, which encodes cyclin D1, are repressed (Richon et al., 2000; Sandor et al., 2000). In addition, HDACi cause hyperacetylation of Hsp90, Raf, Akt, ErbB2 and Bcr-Abl leading to important antitumor effects (Kim et al., 2006). Thus, the transcriptional and non-transcriptional effects of HDACi render this class of molecules attractive for clinical developments in cancer therapy as drugs which target multiple pathways (Bolden et al., 2006; Liu et al., 2006; Smith and Workman, 2009).

Several HDACi are currently in early phase of clinical development as potential treatments for solid and hematological cancers, either as monotherapy or in association with other anticancer agents (Bolden et al., 2006). However, since most of them are insoluble and/or unstable *in vivo* (like trichostatin A – TSA (Elaut et al., 2002; Vanhaecke et al., 2004)) we decided to incorporate them in pegylated liposomes to allow their i.v. administration. Pegylated liposomes (Stealth® property) are second generation devices that, contrary to non-pegylated liposomes, are less rapidly captured by the reticulo-endothelium system (RES) presenting an enhanced pharmacokinetic profile. They take advantage from the enhanced permeability and retention effect (EPR) for increasing their tumor

Abbreviations: HDAC, histone deacetylase; HDACi, HDAC inhibitor; TSA, trichostatin A; ER, estrogen receptor; DSPE-PEG$_{2000}$, 1,2-distearoyl-sn-glycero-3-phosphoethanolamine-*N*-[methoxy(polyethylene glycol)-2000] (ammonium salt); ePC, egg phosphatidylcholine; Chol, cholesterol; MTT, 3-[4,5-dimethylthiazol-2-yl]diphenyltetrazolium bromide.

* Corresponding author at: Centre National de la Recherche Scientifique, UMR 8612, Faculté de Pharmacie, 5 rue J.B. Clément, Châtenay-Malabry, F-92296, France. Tel.: +33 1 46 83 58 31, fax: +33 1 46 83 58 32.
E-mail address: michel.renoir@u-psud.fr (J.-M. Renoir).

0378-5173/$ – see front matter © 2010 Elsevier B.V. All rights reserved.
doi:10.1016/j.ijpharm.2010.06.046

accumulation when they are intravenously injected (Drummond et al., 1999). Such a type of nanocarrier is supposed to improve the pharmacokinetic and pharmacodistribution of the encapsulated drug (Moghimi and Szebeni, 2003).

In the present study, we compared the capacities of pegylated liposomes to load three class I and II HDAC inhibitors (CG1521, PXD101 and TSA), characterized their physicochemical and biological properties and evaluated their toxicity towards several ER-positive and ER-negative human breast cancer cell lines. These formulations revealed to be stable for one month, both in terms of their physicochemical characteristics (size and zeta potential) and of their biological activity *in vitro* (capacity to induce histone H4 acetylation). In addition, they revealed slow drug release kinetics which is fundamental to allow the nanosystem to accumulate in tumor tissues once intravenously injected. These preliminary results encourage further *in vivo* evaluation in appropriate xenograft models.

2. Material and methods

2.1. Chemicals

TSA was obtained from Alomone Labs (Jerusalem, Israel); CG1521 (CG) and PXD101 (belinostat) were obtained from Errant laboratories and Topo Target CuraGen Corp., respectively. They were solubilized in ethanol at 1–3 mM final concentration and stored at −20 °C. EPC and DSPE-PEG_{2000} were purchased from Avanti Polar Lipids (Alabaster, AL, USA); FITC-dextran, MTT tetrazolium salt and Chol were obtained from Sigma Aldrich (St. Quentin-Fallavier, France). Spectra/Por dialysis tubing was obtained from Spectrum Laboratories (Rancho Dominguez, CA, USA). All other chemicals were reagent grade, purchased from standard suppliers.

2.2. Liposome fabrication

Liposome suspensions (50 mM lipids) were prepared by a procedure previously described (Maillard et al., 2005). Lipid film hydration was performed at the following molar ratio: ePC/Chol/DSPE-PEG_{2000} (64:30:6). Incorporation of HDACi in liposomes was obtained by mixing the drugs (from 0.5 to 1.5 mM initial concentration) with chloroformic lipid solution. The lipid film was formed by removing the organic solvent under reduced pressure before being hydrated in Hepes buffer (Hepes 10 mM, NaCl 145 mM, pH 7.4). The resulting multilayer vesicles were then extruded (extruder Whitley, Lipex, Vancouver, Canada) sequentially through 0.2 and 0.1 μm polycarbonate membranes (Millipore, USA). Unincorporated HDACi were eliminated by ultracentrifugation (300,000 × *g* × 14 h at 4 °C; L8-70, Rotor 50.4 Ti, Beckman, USA). For FITC-dextran containing liposomes, the lipid film was hydrated with Hepes buffer containing FITC-dextran (10 mg/mL).

2.3. Physicochemical characterization of liposomes

Liposome size and zeta potential were determined with a Zetasizer 4 Malvern (Malvern Inst., UK) from three independent samples. The concentration of encapsulated HDACi in liposome was determined by UV-spectrophotometry at λ_{max} of 336 nm, 342 nm or 268 nm for CG1521, TSA and PXD101, respectively, after ethanol solubilization of purified drug-loaded liposomes. The drug loading efficiency (DLE) was calculated as follows: DLE1% = amount of drug in purified liposomes/amount of drug initially added × 100 or DLE2% = amount of drug in purified liposomes/amount of drug measured before purification of liposomes × 100.

2.4. Cell culture treatments and transcription measurement

MCF-7, T47-D A 1-2, SKBr-3 and MDA-MB-231 cell lines (ATCC, Molsheim, France) were cultured in Dulbecco's modified Eagle's medium (DMEM, Lonza, Vervier, Belgium) supplemented with penicillin (5 IU/mL), streptomycin (50 IU/mL), 10% fetal calf serum (FCS). MELN cells are MCF-7 cells stably expressing the ERE-βglobin-luciferase construct (Balaguer et al., 1999). Prior to treatment, the medium was replaced with phenol red-free DMEM medium containing 10% stripped FCS (charcoal Norit A 1%, dextran T70 0.1%, 30 min at room temperature) for at least 48 h. For transcription measurements, cells were seeded on 3 cm diameter plates 32 h before treatments in phenol red-free DMEM supplemented with 10% dextran-coated charcoal stripped FCS. Cells were stimulated with 0.1 nM E_2 in the presence or not of various concentrations of either CG, or PXD (0.5–5 μM) or TSA (0.05 to 1 μM) for 16 h, then harvested and lysed in 250 μL of luciferase buffer (25 mM Tris, H_3PO_4 pH 7.8, 10 mM $MgCl_2$, 10% Triton X-100, 15% glycerol, 1 mM EDTA, 1 mM DTT) for 30 min at 4 °C. Luciferase buffer (50 μL), supplemented with 100 mM ATP and 87 μg luciferine/mL, was added to 50 μL of cell extract and luciferase activity was quantified in a luminometer (Lumat LB 9507, Berthold, Bad Wildbad, DE). The protein concentration of each sample was determined by Biorad assay and luciferase activity was normalised with respect to protein concentration.

For measurement of HDACi activity, MCF-7 and MDA-MB-231 cells at 50–60% confluence in 3 cm diameter plates were exposed or not during 20 h to various concentrations of inhibitors (0.05–10 μM). Cells were then lysed in lysis buffer (50 mM Hepes pH 7.5, 150 mM NaCl, 1.5 mM $MgCl_2$, 1 mM EGTA, 10% glycerol, 1% Triton X-100) with protease inhibitors (Complete Reagent, Roche Diagnostics, Indianapolis, IN, USA) for 20 min and then boiled for 10 min in Laemmli sample buffer prior Western blotting (see below).

2.5. In vitro drug release

In a first experiment, drug-encapsulated liposomes (750 μL) were placed into a dialysis tubing (MW cut-off = 10,000 Da), then dialysed against 250-fold excess of Hepes buffer (10 mM Hepes, 0.15 M NaCl, pH 7.4) supplemented with 30% FCS for 24 h at 37 °C. At various times, 50 μL aliquots were removed for drug quantification by spectrophotometry. Physicochemical characteristics of liposomes were further evaluated by quasi-elastic light scattering.

The drug release rates were also determined in MELN cells ($0.5–2 \times 10^6$ cells at 50–60% confluence). Liposomes were placed in inserts (NUNC Anapore, membrane 0.02 μm, Nalge Nunc Inc., USA) with or without 0.1 nM E_2 and the extent of increase of luciferase (LUC) activity was compared to that of equivalent concentrations of free HDACi. Only free HDACi and E_2 could pass through the insert membrane. At different times, inserts were removed from the dishes and cells were maintained at 37 °C for 24 h. LUC activity was quantified as described previously (Maillard et al., 2006).

2.6. In vitro liposome uptake

MCF-7 cells were plated onto a sterile cover-slip paced in 6-well plates and let to adhere for 24 h at 37 °C. Each test was carried out with cells at 50% confluence. FITC-dextran loaded liposomes were added (20 μL) to 3 mL DMEM in each test well for incubation (12 h at 37 °C or 4 °C). For control, cells were treated with free FITC-dextran and incubated similarly. After three washes with cold PBS (10 min), fresh PBS was added and the cover slips were placed on a microscope slide. The slides were then examined using a Nikon eclipse TE2000-S fluorescent microscope (Nikon, Champigny/Marne, France) at ×200 magnitude coupled to a Nikon

DXM 12000C digital camera. Nis-Elements imaging software was used for image processing.

2.7. Cell viability determination

Cells (10^4 cells per well) were seeded into 96-well plates, incubated for 72 h with HDACi-charged liposomes or free HDACi at different concentrations. The MTT tetrazolium component was then added and the plates were incubated for 2 h. Cell medium was then withdrawn, 100 μL of DMSO were added and the absorbance at 570 nm was recorded using a 96-well plate reader (Σ 960, Metertech Inc., Germany).

2.8. Immunobloting

For Western blot analysis, cells were lysed and protein concentration was quantified as already described (Ameller et al., 2003). Protein content from total cell extracts (15–30 μg) was separated by electrophoresis on SDS-PAGE and electrotransferred onto a polyvinylidene difluoride membrane (Immobilon P, Millipore Corp, Saint-Quentin en Yvelines, France). The membrane was blocked for 1 h at 37 °C in 10% dried non fat milk in PBS containing 1% Tween 20 (PBST) and further incubated 45 min at room temperature with anti-ERα (HC-20, 0.1 μg/mL, Santa-Cruz Biotechnology, Santa-Cruz, CA, USA), or anti-acetyl-histone H4 (ref 07-328 from Upstate, Temecaula, CA, USA, at 0.1 μg/mL) or anti-hsp70 (W7, Santa-Cruz, at 0.1 μg/mL). Appropriate horseradish peroxidase-conjugated secondary antibodies (45 min incubation at room temperature) and Luminol reagent (Santa-Cruz) were used for detection.

2.9. Transmission electron microscopy

Liposomes shapes were analyzed through TEM (transmission electron microscope, Philips EM208) at 60 kV. 3 μL of liposome dispersions diluted in Hepes buffer (1/50, v/v) were placed on a formvar-carbon film previously coated on a copper grid (400 meshes). After 5 min of deposition, a drop of phosphotungstic acid was placed on the copper grid, on top of the sample. After 30 s, the liquid was drained and the sample was placed inside the EM208 and pictures were taken.

2.10. Statistical analysis

Student's *t*-test was used for the determination of differences between two experiments. Repeated measures ANOVA test was used for comparisons of curves obtained in experiments related to MTT tests and drug release measures. A value of $p < 0.05$ was considered representative of a significant difference.

3. Results

3.1. In vitro activity of HDACi in breast cancer cells

The activity of HDACi was evaluated in the breast cancer MCF-7 and MDA-MB-231 cell lines. TSA and PXD both induced a dose-dependent and MG132-sensitive degradation of ERα in MCF-7 cells, suggesting a proteasome-mediated degradation, albeit according to various extents. Ten μM CG caused only a weak decrease of ERα (Fig. 1) while TSA and PXD induced a decrease of ERα already at 0.5 and 5 μM, respectively, a process inhibited by MG132. Control experiments showed that TSA was also the strongest inhibitor of HDACs in both breast cancer cells, as revealed by the dose-dependent induced increase in acetylated-histone H4 level, while CG revealed to be a poor inhibitor or was unstable in our experimental conditions (Fig. 1). The potential of the three HDACi to modulate ER-mediated transcription was studied as well in MELN cells as well. As shown in Fig. 2A–C, TSA was the strongest enhancer of the E_2-induced luciferase activity (×250-fold), followed by PXD (×80-fold), while CG had no effect.

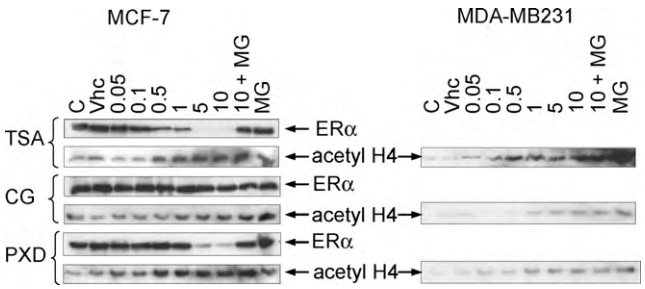

Fig. 1. Biological activities of various HDACi on protein stability in breast cancer cells. MCF-7 and MDA-MB-231 cells were exposed or not (control, C, or vehicle alone, Vh) to increasing concentrations of TSA, CG or PXD during 20 h in the presence or not of 5 μM of the proteasome inhibitor MG132 (MG). ERα was immunoblotted and analyzed by Western blot in 30 μg of protein from total cell extracts as described in Section 2. The detection of acetyl-histone H4 served as a control of the activity of the HDACi.

Thus, TSA appears as the most potent HDACi of the three drugs studied here, both in terms of its effects on acetylated-histone level and on the turnover of a target protein such as ERα. Moreover, CG is likely one compound which does not inhibit the HDAC involved in ERα-mediated transcription, contrary to PXD and mainly TSA.

3.2. Physicochemical parameters and loading efficiency of liposomes

The hand-shaken method used for the preparation of desired liposomes led to small vesicles of ∼100 nm in hydrodynamic diameter (see Table 1). The size of such unloaded liposomes did not significantly varied over a 4-week period when stored at 4 °C under nitrogen. The formulation composed of ePC/CHOL/DSPE-PEG_{2000} was chosen because it resulted already successful for the encapsulation of hydrophobic compounds such as the "pure" antiestrogen RU58668 with a consequent high stability once i.v. injected (Maillard et al., 2005) and Rapamycin (Rouf et al., 2009). Addition of cholesterol was chosen based on previous data from our laboratory (Maillard et al., 2006) and from the literature. Indeed, cholesterol is known to enhance membrane rigidity and compactness, thus rendering lipid bilayer less permeable for encapsulated drugs (Bally et al., 1990; Gabizon, 1993). As well, the addition of a small aliquot of PEG was performed in order to provide steric stabilization of the drug-loaded vesicles, with the objective to improve their circulation half life as widely demonstrated in the past (Allen et al., 1991a; Gabizon and Papahadjopoulos, 1988; Klibanov et al., 1991).

When TSA and PXD were added to the formulation a very slight increase in liposome size (∼150 nm) was noticed although insignificant while CG-loaded liposomes conserved a size of ∼100 nm. This is likely due to the linearity in its chemical structure compared to the presence of an amine group in TSA and a sulphonylamide group in PXD (Table 1). Size and zeta potential measurements were conducted each week over a period of one month. When stored at 4 °C, TSA- and PXD-liposomes, when stored at 4 °C showed no physicochemical changes during this time. Moreover, no modification of the zeta potential of all HDACi-loaded liposomes, compared to unloaded liposomes, was noticeable (ζ ∼20 mV), suggesting that the inhibitors were incorporated within the lipid bilayers and probably not adsorbed on their surface. Importantly, we found that the liposome structure was not affected by the purification method, since no change in size and shape was observed before and after purification of CG and TSA-liposomes (not shown). Fig. 3 revealed a multilamellar structure for all preparations which is the most indicated for encapsulation of a hydrophobic drug (see Moghimi

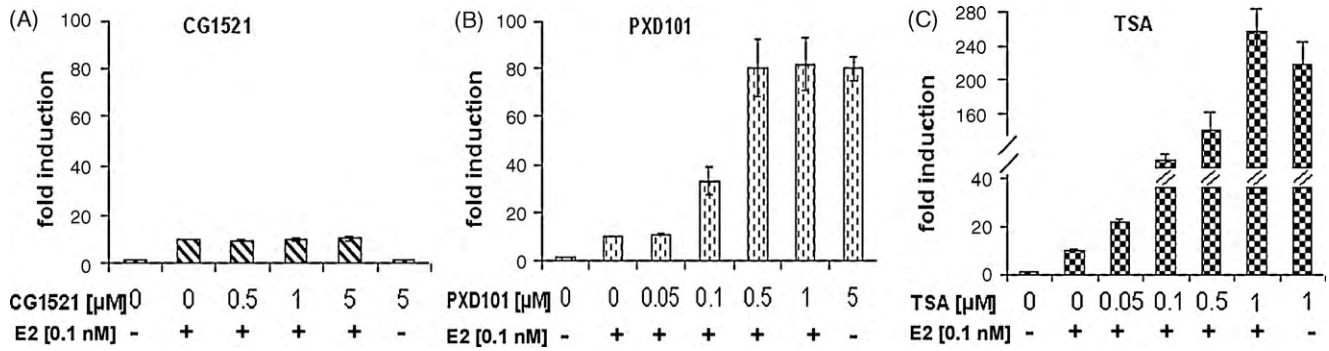

Fig. 2. Capacity of various HDACi to affect ER-mediated transcription in MELN cells. MELN cells were exposed or not to increasing concentrations of the three HDACi in the presence of 0.1 nM E_2, during 20 h. Luciferase was measured as described previously in Section 2 and the increase of luciferase expression (fold induction) was plotted with regard to basal level of transcription obtained in the absence of HDACi (0) affected to a value of 1.

et al., 2001 for a review). The liposome sizes revealed by TEM in Fig. 3 well agreed with those measured by quasi-elastic light scattering (Table 1). No significant difference was noticed for the structure of liposomes both charged and empty, whether before and after purification, similarly to data obtained with the zetasizer (not shown).

The loading efficiency was studied to evaluate the best ratio between the lipid concentration and the amount of drug initially added. Four different concentrations of HDACi were tested and the drug loading yield was analyzed after liposome purification. As shown in Fig. 4, PXD- and CG-loaded liposomes reached the highest encapsulation loading when 1 mM drug was used for their preparation. When initial concentrations rose up to 1.5 mM, the loading efficiently promptly dropped, suggesting a destabilization of the nanocarrier. For initial concentrations of TSA above 1 mM, the encapsulation yield did not increase, resulting in a plateau of drug incorporation. These results led to conclude that the optimal initial drug concentrations to get, on the basis of DLE1 formulae, successful loading of 99 ± 3% (n = 6) for PXD-loaded liposomes, 77 ± 3% for CG-liposomes (n = 4) and 67 ± 4% (n = 11) for TSA-liposomes, respectively, was close to 1 mM indifferently for all three HDACi. The same incubation conditions also resulted in the best loading rates, i.e., of 94% (PXD), 95% (CG) and 75% (TSA) when DLE2 was used. There was no significant difference between DLE1 and DLE2 values for PXD- and CG-liposomes. The apparent low yield for TSA-liposomes should be a limitation in the eventuality of the extension to industrial production due to the cost of TSA.

3.3. Stability of encapsulated HDACi

In a further experiment, we checked for the biological stability of encapsulated HDACi within liposomes. Since the prime biological effect of HDACi is to induce histone acetylation, we measured the capacity of encapsulated HDACi to affect such post-translational activity of histone H4. We focused on TSA-liposomes and incubated MCF-7 cells for 20 h with increased amount of freshly prepared TSA-liposomes or 4 week old TSA-liposomes stored at 4 °C. Fig. 5A shows an enhanced histone H4 acetylation from MCF-7 cells exposed to liposomes-TSA compared to untreated cells, although the dose–response was not obvious. Importantly, the only

Table 1
Physicochemical characteristics and stability of liposomes.

Liposomes physicochemical properties and stability					
	Diameter (nm, mean ± width)				D
	ζ potential (mV, mean ± SD)				ζ
	1 day	1 week	2 weeks	1 month	
Unloaded liposomes	126 ± 31.2 −24.9 ± 7.6			102 ± 25.2 −22.8 ± 5.3	D ζ
lipo-TSA 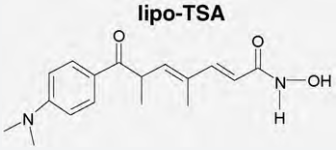	150 ± 38.3 −22.2 ± 7.1	143 ± 36.8 −29.3 ± 9.5	164 ± 23 −22.8 ± 9.4	143 ± 39.5 −19.1 ± 11.2	D ζ
lipo-PXD 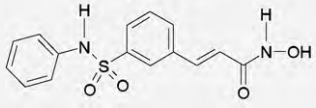	148 ± 39 −24.5 ± 7.9	150 ± 41 −23.1 ± 7.6	150 ± 36.8 −23.2 ± 8.2	148 ± 35.9 −29.6 ± 8.1	D ζ
lipo-CG 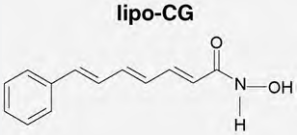	100 ± 23.2 −21.0 ± 7.3	94 ± 20.0 −24.4 ± 8.2	83 ± 25.2 −20.2 ± 8.4	149 ± 33.4 −15.4 ± 7.8	D ζ

Mean diameter (D) and zeta potential (ζ) (±SD) of the three HDACi-liposomal formulations are indicated (n = 3 for three different preparations). Student's t-test statistical analysis revealed no significant differences (p > 0.5) between the values measured at 4 weeks and those measured after 1 day storage.

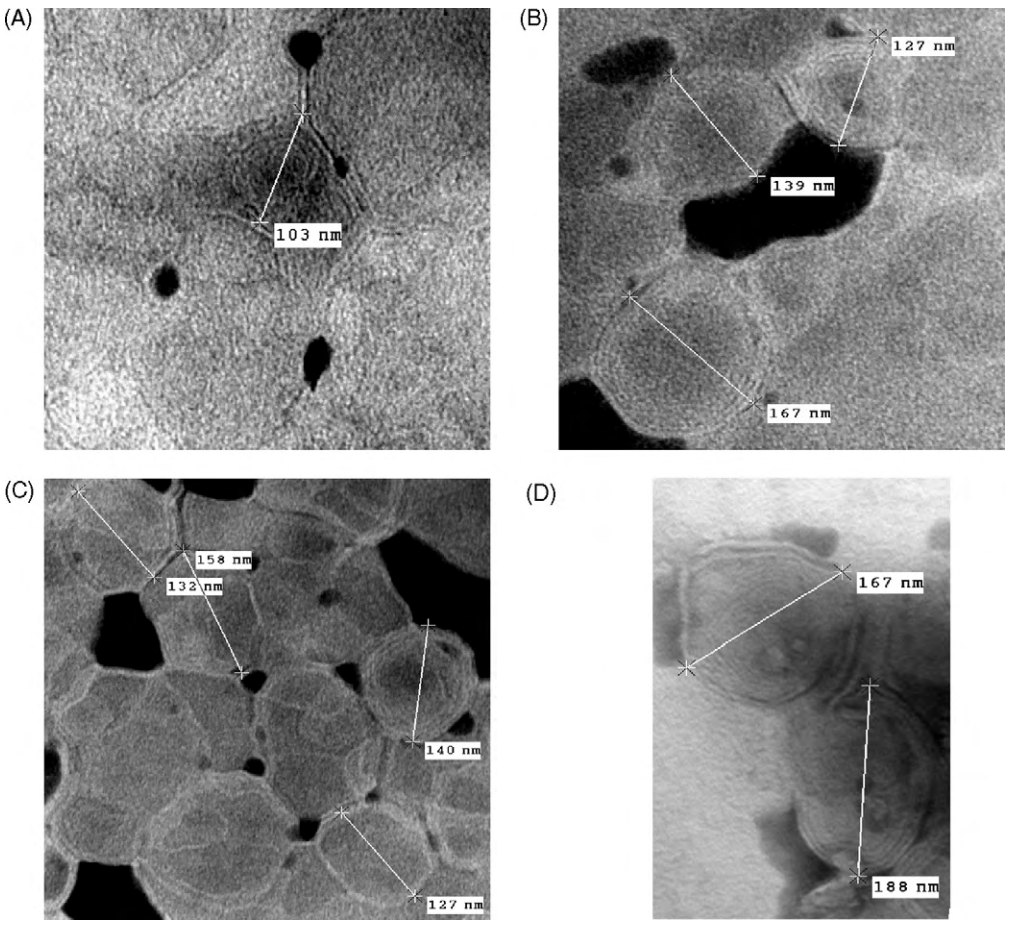

Fig. 3. TEM on empty and charged HDACi-loaded liposomes. Empty liposomes (A) and TSA- (B), PXD- (C), and CG-charged liposomes (D) were visualized by TEM as described in Section 2, respectively. Images clearly show a MLV structure for all preparations, whether after or before (not shown, similar images) purification.

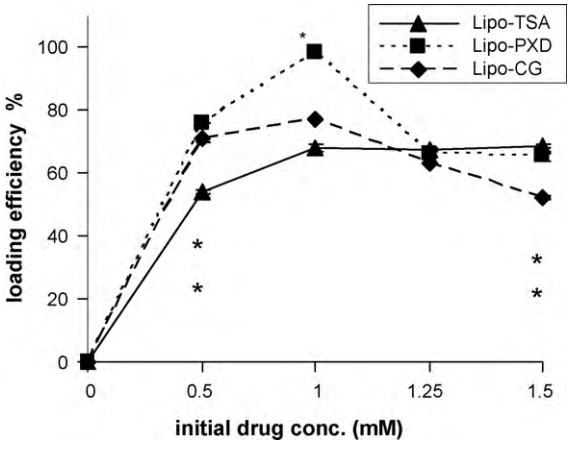

Fig. 4. Loading efficiency of HDACi-liposomes. The incorporated HDACi concentrations or drug-loaded efficiency (DLE) were measured, after various HDACi concentrations (0.5–1.5 mM) have been added to the lipidic films. The different curves represent the DLE calculated for the three different liposomal formulations: TSA-loaded liposomes (lipo-TSA), CG-1521-loaded-liposomes (lipo-CG) and PXD101-loaded liposome (lipo-PXD). Values are the mean of three independent liposome fabrications measured in triplicates. A significant difference was observed by ANNOVA test between all incorporated drugs at 1 mM initial concentrations (*$p < 0.01$) and for incorporated TSA at 0.5 mM and both lipo-PXD and lipo-CG on one hand (**$p < 0.05$), and for 1.5 mM incorporated lipo-CG and both lipo-PXD and lipo-TSA (**$p < 0.05$), on the other hand.

way to observe an effect of TSA-liposomes on a target protein was to use a small volume of culture medium in order to reduce the dilution factor for TSA-liposomes. Indeed, when TSA-liposomes are highly diluted (>1/1000) no effect was observed (not shown). This is explained by the important dispersion of TSA-liposomes in the culture medium, which favors retention of TSA in the liposome bilayer, since the nanodevices remained far from the cells precluding their cellular uptake. At 1/50 dilution (equivalent to 20 μM TSA, TSA-liposomes were better taken up by MCF-7 cells than at higher dilution, as revealed by a stronger signal for acetyl histone H4 than that induced for free TSA. This is consistent with an increased

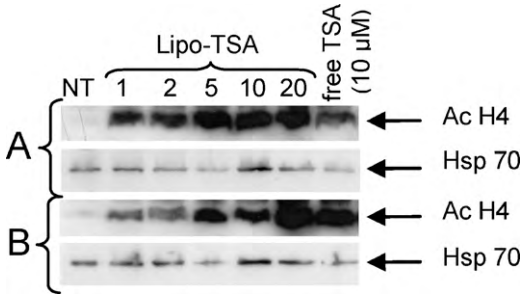

Fig. 5. *In vitro* stability of encapsulated TSA in liposomes. MCF-7 cells (0.5×10^6) in 2 mL of culture medium were exposed or not (NT, not treated) to various concentrations of freshly prepared TSA-liposomes and to 10 μM of TSA (A) or stored 4 weeks at 4 °C (B). After incubations, cells were harvest, washed and total cell extracts (15 μg proteins) were separated on 15% SDS-PAGE, blotted as described in Section 2 with the anti-acetyl H4-histone antibody. After stripping of the same blot, hsp70 was probed for control of constant protein loading.

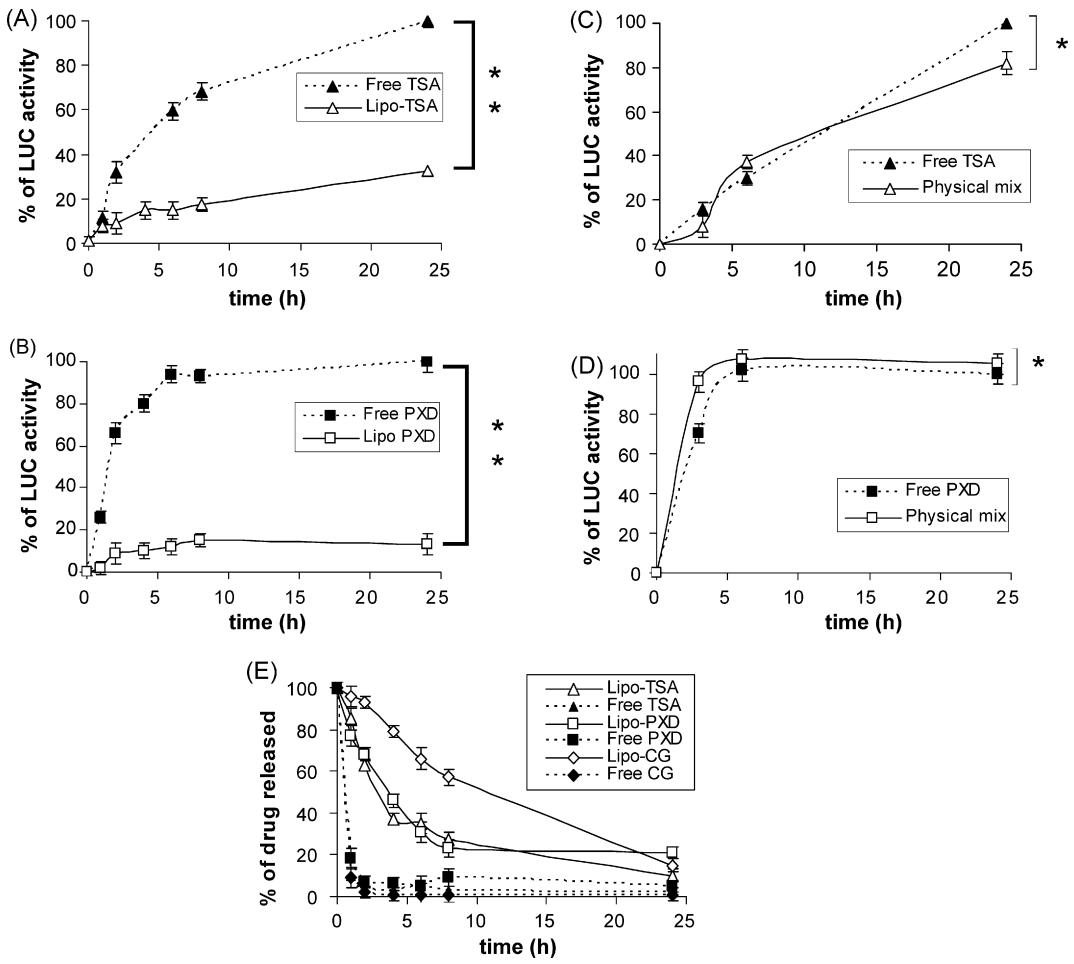

Fig. 6. *In vitro* release kinetic of liposome incorporating HDACi. In panels A and B, the level of luciferase expressed in MELN cells following exposure to either free or encapsulated HDACi is shown. Free HDACi or liposomal-HDACi were loaded in inserts with 0.1 nM E_2 and LUC activity was measured after different times of incubation, corresponding to the time at which inserts were removed. One hundred percent of transcription corresponds to the level of LUC measured after 24 h exposure to E_2 in presence of the maximum amount of free HDACi. ANOVA test indicated a significant difference between the two curves in each panel A and B ($^{**}p < 0.001$). In panels C and D, TSA or PXD at an equivalent concentration to that encapsulated for each formulation used in panels A and B, were mixed to empty liposomes (physical mix) or not, then luciferase activity was measured. Statistical ANOVA test did not revealed any significant difference ($^{*}p > 0.5$) between the two C and D curves. In panel E, released HDACi incorporated or not (free HDACi) in liposomes were measured by spectrophotometry following the dialysis experiment, after various times of dialysis. One hundred percent corresponds to the amount of incorporated HDACi before dialysis. Statistical analysis revealed no significance (ANOVA test) between the release kinetics of the three free drugs, but revealed a significant slow down of the release kinetics of all encapsulated molecules as compared to that of the free drugs ($p < 0.01$). Additionally, a significant decrease of release kinetics was measured between the encapsulated CG vs encapsulated PXD and encapsulated TSA ($p < 0.01$) for times below 10 h.

uptake of TSA-liposome by cells. The biological activity of encapsulated TSA persists after 4-week storage of the TSA-liposomes (Fig. 5B) since histone H4 acetylation is still enhanced by the 4-week-old TSA-liposomes. This is consistent with the preservation of the enzymatic activity of encapsulated TSA, in concordance with the preservation of the physicochemical parameters of the liposomes. We emphasize that data with other encapsulated HDACi would have been similar in terms of the preservation of the biological activity of trapped inhibitors; indeed, other experiments not mentioned here were performed with formulations stored at 4 °C in order to check for the activity of encapsulated HDACi on E_2-induced transcription in MELN cells, as well as on the fate of proteins such as cyclin D1 and Rho-B GTPase known to be targets of HDAC inhibition (manuscript in preparation).

3.4. *In vitro* drug release kinetics

Fig. 6 shows the release kinetics of the encapsulated HDACi from liposomes measured by two different ways, a biological study comparing the ability of free and released HDACi to enhance transcription in MELN cells (Fig. 6A–D) and a physical method using dialysis of the HDACi-loaded liposomes against buffer supplemented with FCS (Fig. 6E). In the experiment using MELN cells, only TSA and PXD were assayed since CG had no effect on E_2-induced transcription in MELN cells (Fig. 2). TSA released from liposomes increased the E_2-induced transcription in MELN cells only by 30% after 24 h (Fig. 6A) and PXD only by 15% (Fig. 6B), compared to free compounds which induced transcription by 100% at this time. These differences suggest a slow release of the encapsulated drugs. A further study was then performed to verify that these differences between the activities of free and encapsulated HDACi were strictly related to the entrapment of the molecules inside the liposomes. Noteworthy, Fig. 6C and D showed that no difference between the ability of the HDACi alone to affect transcription and that of a physical mix of unloaded liposomes plus free HDACi was found, respectively. These data strongly support the fact that a physical contact between HDACi and liposomes such as in the case of the physical mix is not sufficient to change the pharmacokinetic profile of the drug(s). As a consequence, they also suggest that the drugs must be buried in the lipid bilayers, a feature compatible with their slow release from the liposomes.

Table 2
Free and encapsulated HDACi antiproliferative activities in breast cancer cell lines.

IC50 (μM)			
Samples	Cell lines		
	MCF-7	MDA-MB-231	SKBr-3
Lipo-TSA	0.34 ± 0.02	0.42 ± 0.02	0.20 ± 0.01
Free-TSA	0.08 ± 0.001	0.09 ± 0.003	0.05 ± 0.02
Lipo-PXD	0.72 ± 0.05	0.33 ± 0.04	5.00 ± 0.25
Free-PXD	0.60 ± 0.05	0.50 ± 0.04	5.00 ± 0.25
Lipo-CG	9.60 ± 0.40	5.50 ± 0.3	5.00 ± 0.25
Free-CG	6.50 ± 0.25	3.40 ± 0.2	5.00 ± 0.25

IC_{50} (mean of height values from two separate experiments ± SD) was defined as the drug concentration that inhibits cell growth by 50% compared to untreated cells. Values represent data extrapolated from curves from Fig. 7.

Since the experiments from Fig. 6A and B did not allow to assess for the release of encapsulated CG, we turned to the classical dialysis method to evaluate this parameter, although it does not reflect exactly the *in vivo* conditions. Fig. 6E demonstrated that the release rate of encapsulated CG occurred slower than that of TSA and PXD. This behavior can be explained by its more lipophylic chemical structure that favors interactions with lipids (Table 1). TSA- and PXD-liposomes releases were similar and faster than that of CG, but slower than that of free drugs. As noted above, the additional NH_2-group in TSA and the sulfonamide group in PXD confer better water solubility to these molecules which tend to escape faster from liposome bilayers, according to better amphiphile-like behavior than purely lipophilic molecules do (Gulati et al., 1998). In controls, 80% of free drugs were released already after 2 h, reaching 96% after 4 h, whereas liposomes retained nearly ~50% from the first 4 h and still 20% after 24 h.

Taken together, the results from Fig. 6 and stability experiments indicate that HDACi are slowly released from liposomes, a prerequisite for conducting further *in vivo* evaluations.

3.5. Cytotoxicity of HDACi-loaded PEG-liposomes

The cytotoxicity of the three HDACi and of their relative liposomal formulations was measured over a panel of different cancer cell lines representing various typology of breast cancer disease. Unloaded liposomes were evaluated as well to ensure the non-toxicity of the empty vehicle. As shown in Fig. 7, they exhibit a very weak toxicity since 90% of cell viability was measured for all cell lines after 72 h exposure even at the highest concentration. TSA was the strongest inhibitor of cell viability in all cell lines tested, followed by PXD and by CG, with IC_{50} varying from ~0.1–0.5 μM for TSA to 1–10 μM for PXD and CG, depending on the cell line (Table 2). However, encapsulated HDACi, principally TSA, were less efficient than free HDACi. Thus, encapsulated drugs revealed important anticancer activity although lower than that of free drugs in accordance with a retarded effect due to retention phenomenon, more obvious at low concentrations.

3.6. In vitro liposome uptake

In order to see if free or liposome-trapped drug could accumulate at the same rate in cancer cells, MCF-7 cells were exposed to either free or FITC-dextran-loaded liposomes then analyzed by fluorescence microscopy. Fig. 8 indicated that, at 37 °C, free FITC-dextran did not label any cell, contrary to FITC-dextran-loaded liposomes which induced a punctiform fluorescence accumulation in the cytoplasm of cells. Control experiments performed at 4 °C, a temperature known to block endocytosis (Dunn et al., 1980) revealed no fluorescence in cells. Similar work was performed previously with the same formulation of ePC/Chol/DSPE-PEG labeled

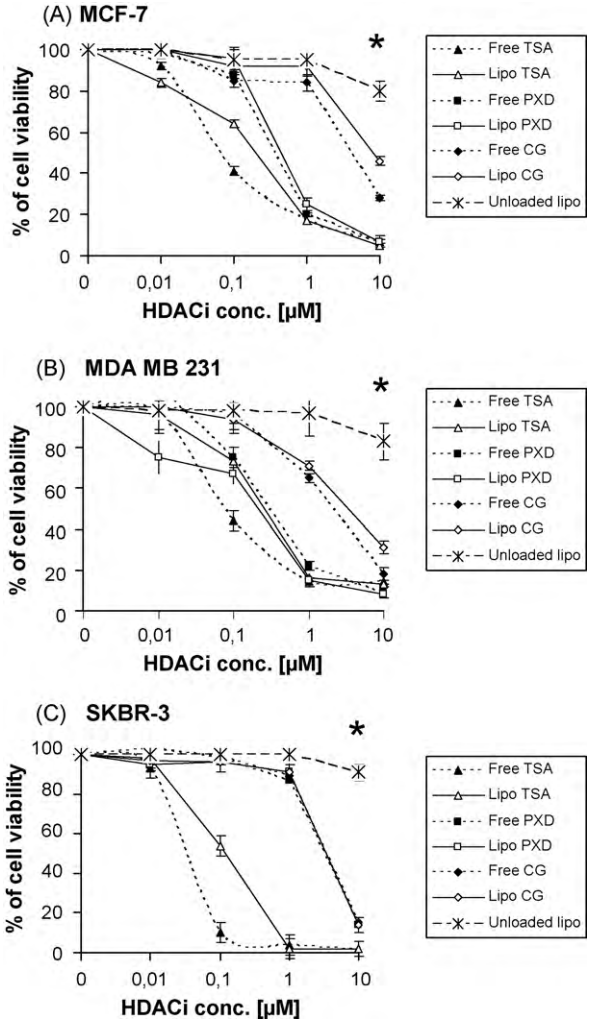

Fig. 7. Breast cancer cells viability upon exposure to HDACi. MCF-7 ER-positive cells (A), MDA-MB-231 ER-negative cells (B) and SKBR-3 ER-negative and Erb-B2-positive (C) cells were incubated or not (vehicle only) for 72 h (two cell-doubling times) with various concentrations of either free or lipo-HDACi. The number of viable cells was measured by the MTT test (100% corresponds to the number of viable cells incubated with ethanol only). Results are the mean ± SD ($n = 8$). At liposome amount equivalent to 10 μM TSA, empty liposomes showed an un-significant ($p > 0.05$) low toxicity at 72 h, 80–90% cells remaining still viable. This toxicity was strongly enhanced for both free HDACi and HDACi-loaded liposomes from the same species, when compared to empty liposomes, as revealed by ANOVA test analysis ($p < 0.05$); however no significant difference was noted between free HDACi and corresponding charged liposome ($p > 0.1$).

with Rhodamine-phosphoethanolamine (Rho-PE) (Maillard et al., 2006). It was shown that the same Rho-PE-labelled liposomes were captured by multiple myeloma cells at 37 °C but not at 4 °C. Taken together, the results of Maillard et al. and those from our present work, suggest that liposomes promote the cell internalization of both a molecule trapped within the multilayers of liposomes and other large hydrophilic molecules such as FITC-dextran through an endocytosis-mediated process.

4. Discussion

A number of HDACi have shown a low toxicity *in vivo* in animal models; however, their multisite of action could impose some cautious for their use. Thus, a targeted delivery to desired tissues is recommended to enhance their accumulation at the tumor site and protect them in the blood streams until they reach their site of action. In the present work, we incorporated three poor water sol-

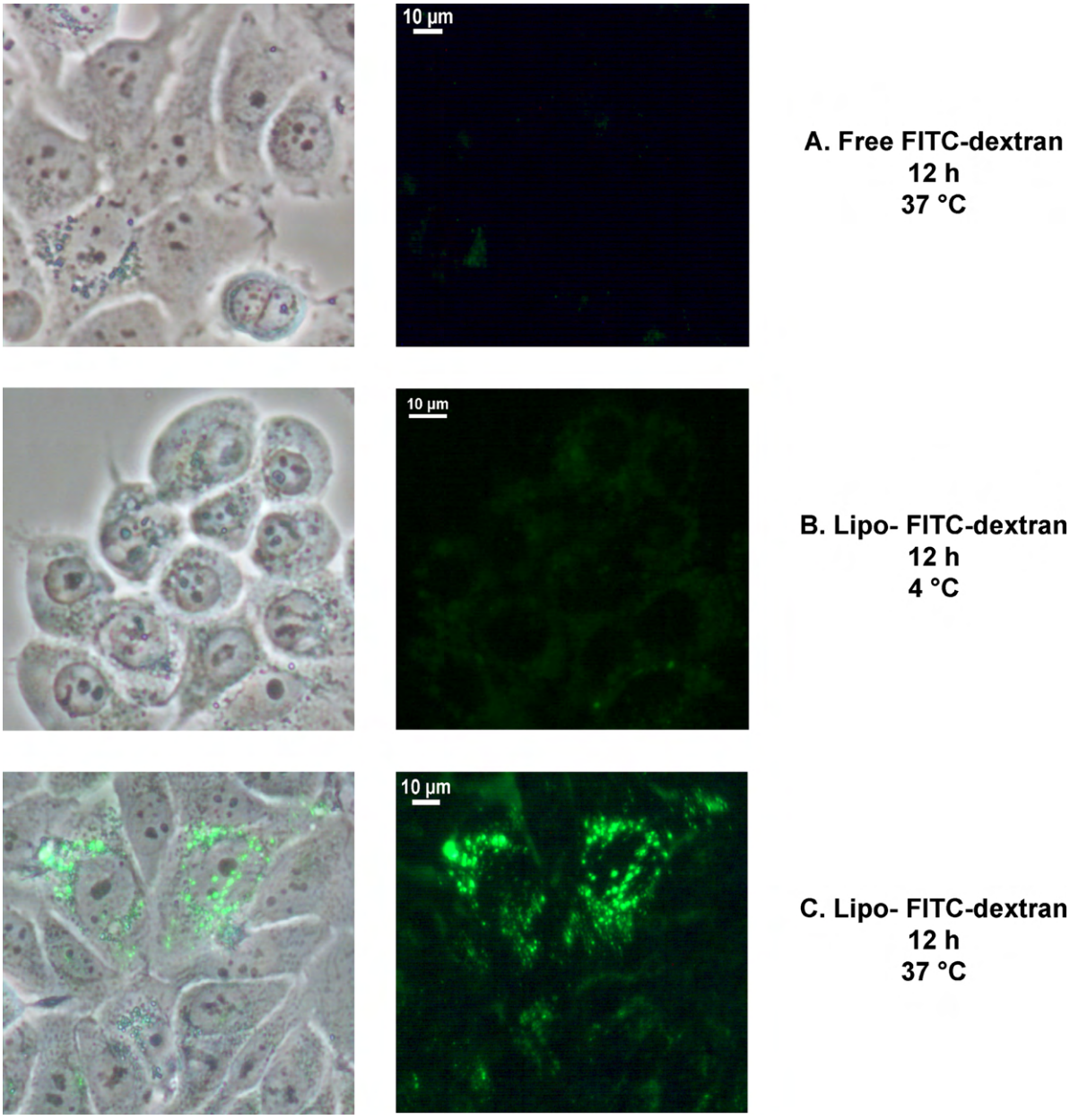

Fig. 8. Uptake of fluorescent labeled liposomes. MCF-7 cells were incubated at 37 °C for 12 h with either free FITC-dextran (A) or Lipo-FITC-dextran (C), at an equivalent fluorescent-dextran concentration (10 mg/mL). In a control experiment (B), cells were incubated at 4 °C in order to block endocytosis process. Images in fluorescence are shown on the right panels. Projections of FITC-fluorescent images (green) superimposed with MCF-7 cells Nomarski image are shown on panels on the left.

uble HDACi in a biodegradable lipid nanocarrier which revealed a multilamellar structure by TEM experiments. At least 4-week stability was observed for the physicochemical parameters of each formulation as well as for the biological activity of encapsulated molecules as exemplified here by encapsulated TSA.

A weak toxicity *in vitro* in multiple myeloma cell lines as well as in xenografts has already been noticed for the same type of empty liposomes (Maillard et al., 2006) and Fig. 7 also demonstrated a low breast cancer cell toxicity. All three inhibitors were encapsulated at high concentrations, reaching 1 mM far above their water solubility, and were released slowly from the pegylated liposomes. Although TSA-liposomes presented the less attractive encapsulation yield, due to the strong antiproliferative activity of TSA itself *in vitro*, very low concentrations are needed to be active *in vivo*. Thus, although it is always difficult to extrapolate from *in vitro* data for *in vivo* therapeutic success, it is expected that this liposomal formulation of TSA could be of clinical interest. Indeed, TSA inhibits numerous zinc-dependent, class I and II HDACs, with an $IC_{50} \leq 0.5\ \mu M$ depending on the HDAC (Bolden et al., 2006). Such IC_{50} values imply that doses far above its solubility are needed to produce a therapeutic effect. At the molecular level, the decrease of ERα in MCF-7 tumor cells treated by TSA, is in agreement with the suppression of E_2-induced tumor growth as suggested by experiments performed with breast cancer cells (Margueron et al., 2003) and colon cancer cells (Archer et al., 1998). Free TSA was the most efficient of the three HDACi tested in breast cancer cell lines, but since this compound has been reported to be unstable *in vivo* following i.v. injection in mice (Elaut et al., 2002; Vanhaecke et al., 2004), its liposomal formulation warrants *in vivo* experiments in animal models to be undertaken. The advantage of TSA-liposomes results from the preserved biological activity of the encapsulated drug. Indeed, it is well established that colloidal particles have a great potential as vehicles for i.v. drug delivery, especially for lipophilic molecules (Gulati et al., 1998). As revealed by cytotoxic-

ity experiments, the unloaded ePC/Chol/DSPE-PEG$_{2000}$ formulation did not demonstrate too much detrimental effect on three different breast cancer cell lines (Fig. 7). Similarly, the low toxicity of other types of liposomes has been well described by others (Drummond et al., 1999; Torchilin, 2007; Working and Dayan, 1996).

CG revealed to be the weakest HDACi in breast cancer cells, but since it is now evaluated in clinical trials against neuroblastomas (de Ruijter et al., 2004) and prostate cancer (in association with the anti-androgen Casodex® (Roy et al., 2005), its liposomal formulation could also enhance its therapeutic activity. Similarly, PXD is developed in clinical trials against hematological cancers such as multiple myeloma and also against solid tumors. Its encapsulation in liposomes could be of clinical interest to improve its delivery in the target cancer cells, favoring its bioavailability and its antitumor capacities.

All these formulated HDACi are easy to prepare at the laboratory scale and stable in storage conditions we used. However, for preclinical and other larger-scale goals, equivalent preparations will be probably substantially more difficult to obtain, with many parameters and characterizations to consider.

Liposomes of such a small size are known to extravasate from capillaries which are often discontinuous in solid tumors (Yuan et al., 1994). Once in tumors, the nanocarrier can be either endocyted, releasing the entrapped active molecule inside the cell compartment, or destroyed outside the tumor cell, releasing the drug which can then diffuse through the cell membrane and thereafter reach the molecular target(s). The endocytosis capacity of MCF-7 is low as compared to multiple myeloma cells exposed to the same PEG-liposomes as shown previously (Maillard et al., 2006). However, these cells are able to proceed to endocytosis as suggested in Fig. 8.

Moreover, since HDACi also block angiogenesis of endothelial cells (Kim et al., 2001) and enhance tumor suppressor gene expression, their accumulation in tumors could enhance their antitumor potential through the inhibition of tumor vasculature. In addition, to improve their cancer cell selectivity, the liposomal formulations could be chemically modified for an active targeting by grafting Erb-B2 antibodies to specifically recognize resistant breast cancer tumors as recently performed for another HDACi, LAQ824 (Drummond et al., 2005). Their co-administration with antiestrogen such as tamoxifen could improve their antitumor efficacy due to the capacity of TSA to restore tumor suppressor expression like ERβ (Jang et al., 2004) and the GTPase Rho-B (Couderc et al., 2008; Durkin et al., 2007).

5. Conclusion

In conclusion, TSA was confirmed to be one of the most potent HDAC inhibitor *in vitro* and could be reconsidered as a molecule of interest *in vivo* thank to an appropriate delivery system able to protect the drug from its fast metabolism occurring after i.v. administration. Moreover, such a delivery system should lead to a decrease of the administered doses and to diminish their frequency, while preserving TSA antitumor activity. Liposomes, because of their well known biocompatibility and tolerability (Allen et al., 1991b) can overcome toxic and irritating effects of standard TSA vehicles like DMSO sometimes used for i.p. administration in animal models (Nishimura et al., 1988). Finally, the preliminary results obtained with all three HDACi liposomal formulations encourage further evaluation of their antitumor activity in appropriate animal models.

Acknowledgements

We deeply thank N. Wiech (Errant), the NCI and Topo Target CuraGen for the generous gifts of CG1521 and PXD101, respectively. We would particularly thank Dr. J. Mester and Pr. A. Gouyette for reading of the manuscript and thoughtful suggestions. We also thank D. Jaillard for TEM analyzes. Financial support was obtained from the Centre National de la Recherche Scientifique, the Université Paris-Sud and the Hauts-de-Seine committee from the Ligue Nationale contre le Cancer (grants to J-M R and fellowship to GU).

References

Allen, T.M., Austin, G.A., Chonn, A., Lin, L., Lee, K.C., 1991a. Uptake of liposomes by cultured mouse bone marrow macrophages: influence of liposome composition and size. Biochim. Biophys. Acta 1061, 56–64.

Allen, T.M., Hansen, C., Martin, F., Redemann, C., Yau-Young, A., 1991b. Liposomes containing synthetic lipid derivatives of poly(ethylene glycol) show prolonged circulation half-lives in vivo. Biochim. Biophys. Acta 1066, 29–36.

Ameller, T., Marsaud, V., Legrand, P., Gref, R., Renoir, J.M., 2003. In vitro and in vivo biologic evaluation of long-circulating biodegradable drug carriers loaded with the pure antiestrogen RU 58668. Int. J. Cancer 106, 446–454.

Archer, S.Y., Meng, S., Shei, A., Hodin, R.A., 1998. p21(WAF1) is required for butyrate-mediated growth inhibition of human colon cancer cells. Proc. Natl. Acad. Sci. U.S.A. 95, 6791–6796.

Balaguer, P., Francois, F., Comunale, F., Fenet, H., Boussioux, A.M., Pons, M., et al., 1999. Reporter cell lines to study the estrogenic effects of xenoestrogens. Sci. Total Environ. 233, 47–56.

Bally, M.B., Nayar, R., Masin, D., Hope, M.J., Cullis, P.R., Mayer, L.D., 1990. Liposomes with entrapped doxorubicin exhibit extended blood residence times. Biochim. Biophys. Acta 1023, 133–139.

Bolden, J.E., Peart, M.J., Johnstone, R.W., 2006. Anticancer activities of histone deacetylase inhibitors. Nat. Rev. Drug Discov. 5, 769–784.

Couderc, B., Pradines, A., Rafii, A., Golzio, M., Deviers, A., Allal, C., et al., 2008. In vivo restoration of RhoB expression leads to ovarian tumor regression. Cancer Gene Ther. 15, 456–464.

de Ruijter, A.J., Kemp, S., Kramer, G., Meinsma, R.J., Kaufmann, J.O., Caron, H.N., et al., 2004. The novel histone deacetylase inhibitor BL1521 inhibits proliferation and induces apoptosis in neuroblastoma cells. Biochem. Pharmacol. 68, 1279–1288.

Drummond, D.C., Marx, C., Guo, Z., Scott, G., Noble, C., Wang, D., et al., 2005. Enhanced pharmacodynamic and antitumor properties of a histone deacetylase inhibitor encapsulated in liposomes or ErbB2-targeted immunoliposomes. Clin. Cancer Res. 11, 3392–3401.

Drummond, D.C., Meyer, O., Hong, K., Kirpotin, D.B., Papahadjopoulos, D., 1999. Optimizing liposomes for delivery of chemotherapeutic agents to solid tumors. Pharmacol. Rev. 51, 691–743.

Dunn, W.A., Hubbard, A.L., Aronson Jr., N.N., 1980. Low temperature selectively inhibits fusion between pinocytic vesicles and lysosomes during heterophagy of 125I-asialofetuin by the perfused rat liver. J. Biol. Chem. 255, 5971–5978.

Durkin, M.E., Yuan, B.Z., Zhou, X., Zimonjic, D.B., Lowy, D.R., Thorgeirsson, S.S., et al., 2007. DLC-1:a Rho GTPase-activating protein and tumour suppressor. J. Cell. Mol. Med. 11, 1185–1207.

Elaut, G., Torok, G., Vinken, M., Laus, G., Papeleu, P., Tourwe, D., et al., 2002. Major phase I biotransformation pathways of Trichostatin a in rat hepatocytes and in rat and human liver microsomes. Drug Metab. Dispos. 30, 1320–1328.

Gabizon, A., 1993. Tailoring liposomes for cancer drug delivery: from the bench to the clinic. Ann. Biol. Clin. (Paris) 51, 811–813.

Gabizon, A., Papahadjopoulos, D., 1988. Liposome formulations with prolonged circulation time in blood and enhanced uptake by tumors. Proc. Natl. Acad. Sci. U.S.A. 85, 6949–6953.

Grunstein, M., 1997. Histone acetylation in chromatin structure and transcription. Nature 389, 349–352.

Gulati, M., Grover, M., Singh, S., Singh, M., 1998. Lipophilic drug derivatives in liposomes. Int. J. Pharm. 165, 129–168.

Huang, L., Sowa, Y., Sakai, T., Pardee, A.B., 2000. Activation of the p21WAF1/CIP1 promoter independent of p53 by the histone deacetylase inhibitor suberoylanilide hydroxamic acid (SAHA) through the Sp1 sites. Oncogene 19, 5712–5719.

Jang, E.R., Lim, S.J., Lee, E.S., Jeong, G., Kim, T.Y., Bang, Y.J., et al., 2004. The histone deacetylase inhibitor trichostatin A sensitizes estrogen receptor alpha-negative breast cancer cells to tamoxifen. Oncogene 23, 1724–1736.

Kim, M.S., Kwon, H.J., Lee, Y.M., Baek, J.H., Jang, J.E., Lee, S.W., et al., 2001. Histone deacetylases induce angiogenesis by negative regulation of tumor suppressor genes. Nat. Med. 7, 437–443.

Kim, T.Y., Bang, Y.J., Robertson, K.D., 2006. Histone deacetylase inhibitors for cancer therapy. Epigenetics 1, 14–23.

Klibanov, A.L., Maruyama, K., Beckerleg, A.M., Torchilin, V.P., Huang, L., 1991. Activity of amphipathic poly(ethylene glycol) 5000 to prolong the circulation time of liposomes depends on the liposome size and is unfavorable for immunoliposome binding to target. Biochim. Biophys. Acta 1062, 142–148.

Liu, T., Kuljaca, S., Tee, A., Marshall, G.M., 2006. Histone deacetylase inhibitors: multifunctional anticancer agents. Cancer Treat. Rev. 32, 157–165.

Maillard, S., Ameller, T., Gauduchon, J., Gougelet, A., Gouilleux, F., Legrand, P., et al., 2005. Innovative drug delivery nanosystems improve the anti-tumor activity in vitro and in vivo of anti-estrogens in human breast cancer and multiple myeloma. J. Steroid Biochem. Mol. Biol. 94, 111–121.

Maillard, S., Gauduchon, J., Marsaud, V., Gouilleux, F., Connault, E., Opolon, P., et al., 2006. Improved antitumoral properties of pure antiestrogen RU 58668-

loaded liposomes in multiple myeloma. J. Steroid Biochem. Mol. Biol. 100, 67–78.
Margueron, R., Licznar, A., Lazennec, G., Vignon, F., Cavailles, V., 2003. Oestrogen receptor alpha increases p21(WAF1/CIP1) gene expression and the antiproliferative activity of histone deacetylase inhibitors in human breast cancer cells. J. Endocrinol. 179, 41–53.
Marks, P.A., Richon, V.M., Rifkind, R.A., 2000. Histone deacetylase inhibitors: inducers of differentiation or apoptosis of transformed cells. J. Natl. Cancer Inst. 92, 1210–1216.
Moghimi, S.M., Hunter, A.C., Murray, J.C., 2001. Long-circulating and target-specific nanoparticles: theory to practice. Pharmacol. Rev. 53, 283–318.
Moghimi, S.M., Szebeni, J., 2003. Stealth liposomes and long circulating nanoparticles: critical issues in pharmacokinetics, opsonization and protein-binding properties. Prog. Lipid Res. 42, 463–478.
Nightingale, K.P., O'Neill, L.P., Turner, B.M., 2006. Histone modifications: signalling receptors and potential elements of a heritable epigenetic code. Curr. Opin. Genet. Dev. 16, 125–136.
Nishimura, M., Takano, Y., Toshitani, S., 1988. Systemic contact dermatitis medicamentosa occurring after intravesical dimethyl sulfoxide treatment for interstitial cystitis. Arch. Dermatol. 124, 182–183.
Richon, V.M., Sandhoff, T.W., Rifkind, R.A., Marks, P.A., 2000. Histone deacetylase inhibitor selectively induces p21WAF1 expression and gene-associated histone acetylation. Proc. Natl. Acad. Sci. U.S.A. 97, 10014–10019.
Rouf, M.A., Vural, I., Renoir, J.M., Hincal, A.A., 2009. Development and characterization of liposomal formulations for rapamycin delivery and investigation of their antiproliferative effect on MCF7 cells. J. Liposome Res. 19, 322–331.
Roy, S., Packman, K., Jeffrey, R., Tenniswood, M., 2005. Histone deacetylase inhibitors differentially stabilize acetylated p53 and induce cell cycle arrest or apoptosis in prostate cancer cells. Cell Death Differ. 12, 482–491.
Sandor, V., Senderowicz, A., Mertins, S., Sackett, D., Sausville, E., Blagosklonny, M.V., et al., 2000. P21-dependent g(1)arrest with downregulation of cyclin D1 and upregulation of cyclin E by the histone deacetylase inhibitor FR901228. Br. J. Cancer 83, 817–825.
Smith, K.T., Workman, J.L., 2009. Histone deacetylase inhibitors: anticancer compounds. Int. J. Biochem. Cell Biol. 41, 21–25.
Torchilin, V.P., 2007. Targeted pharmaceutical nanocarriers for cancer therapy and imaging. AAPS J. 9, E128–E147.
Vanhaecke, T., Papeleu, P., Elaut, G., Rogiers, V., 2004. Trichostatin A-like hydroxamate histone deacetylase inhibitors as therapeutic agents: toxicological point of view. Curr. Med. Chem. 11, 1629–1643.
Vigushin, D.M., Ali, S., Pace, P.E., Mirsaidi, N., Ito, K., Adcock, I., et al., 2001. Trichostatin A is a histone deacetylase inhibitor with potent antitumor activity against breast cancer in vivo. Clin. Cancer Res. 7, 971–976.
Wade, P.A., Pruss, D., Wolffe, A.P., 1997. Histone acetylation: chromatin in action. Trends Biochem. Sci. 22, 128–132.
Working, P.K., Dayan, A.D., 1996. Pharmacological-toxicological expert report. CAELYX. (Stealth liposomal doxorubicin HCl). Hum. Exp. Toxicol. 15, 751–785.
Yuan, F., Leunig, M., Huang, S.K., Berk, D.A., Papahadjopoulos, D., Jain, R.K., 1994. Microvascular permeability and interstitial penetration of sterically stabilized (stealth) liposomes in a human tumor xenograft. Cancer Res. 54, 3352–3356.